EUROPEAN ORGANIZATION FOR NUCLEAR RESEARCH

CERN-EP/81-116
18 September 1981

ASSOCIATED HADRONIC PRODUCTION IN μ-PAIR EVENTS AT THE CERN INTERSECTING STORAGE RINGS

D. Antreasyan[2], W. Atwood[3], U. Becker[3], G. Bellettini[5], P.L. Braccini[5], J.G. Branson[3], J.D. Burger[3], F. Carbonara[4], R. Carrara[5], R. Castaldi[5], V. Cavasinni[5*], F. Cervelli[5], M. Chen[3], G. Chiefari[4], T. Del Prete[5], E. Drago[4], M. Fujisaki[3], M.F. Hodous[3], T. Lagerlund[3], P. Laurelli[5], O. Leistam[1], D. Luckey[3], M.M. Massai[5], T. Matsuda[3], L. Merola[4], M. Morganti[5], M. Napolitano[4], H. Newman[2], D. Novikoff[3], J.A. Paradiso[3], L. Perasso[1], K. Reibel[1**], R. Rinzivillo[4], G. Sanguinetti[1], I. Schulz[3], G. Sciacca[4], P. Spillantini[***], M. Steuer[3], S. Sugimoto[3], W. Toki[3], M. Valdata-Nappi[5], C. Vannini[5], F. Vannucci[3†], F. Visco[4] and S.L. Wu[3††]

1) CERN, Geneva, Switzerland.
2) Physics Department, Harvard Univ., Cambridge, Mass., USA.
3) MIT, Cambridge, Mass., USA.
4) Istituto di Fisica Sperimentale dell'Università and Istituto Nazionale di Fisica Nucleare, Naples, Italy.
5) Istituto di Fisica dell'Università, Scuola Normale Superiore, and Istituto Nazionale di Fisica Nucleare, Pisa, Italy.

(Submitted to Nuclear Physics)

---

*) Now at the Istituto di Fisica dell'Università, Bologna, Italy.
**) Now at the High-Energy Physics Lab., Ohio State Univ., Columbus, Ohio, USA.
***) Laboratori Nazionali di Frascati dell'INFN, Frascati, Italy.
†) Now at Lab. de Physique des Particules, Annecy-le-Vieux, France.
††) Now at the Physics Dept., Univ. of Wisconsin, Madison, Wis., USA.

ABSTRACT

We have measured at $\sqrt{s}$ = 62 GeV, at the CERN Intersecting Storage Rings, the associated charged hadrons with massive μ pairs, employing a vertex detector of $\sim 4\pi$ coverage. The average associated charged multiplicity $\langle n_{ch} \rangle$ is found to increase as the invariant hadronic mass M_h increases, similarly to the observed $\sqrt{s}$ dependence in e^+e^- annihilation at high energies. The multiplicity also increases with the p_T of the dimuon, and this effect can be explained by the production of a weakly collimated jet of low multiplicity.

INTRODUCTION

Massive μ pairs in high-energy hadron interactions have been studied extensively since the J discovery [1], primarily as a search for bound states of new quarks heavier than charm. After the success in the observation of Υ particle [2], the next natural candidate is $t\bar{t}$, the twin state to the Υ in the quark classification models. An upper limit for $\sigma \cdot B_{\mu\mu}$ for this new state was previously obtained by us at the highest ISR energies [3]. On the other hand, non-resonant massive lepton pair production is of interest in itself. First the cross-section and its s-dependence could be compared with the Drell-Yan model of quark and antiquark annihilation into a lepton pair [4]. This model predicts a scaling cross-section in the variable $\tau = m^2_{\mu\mu}/s$ and gives an explicit expression for the lepton pair momentum distributions in terms of quark and antiquark structure functions inside the primary hadrons. These structure functions measured in pp collisions can be compared with those measured in deep inelastic electron and neutrino scattering on nucleons. At ISR energies, the measured proton structure functions are found to be consistent with deep inelastic scattering results [5].

Although the Drell-Yan model is qualitatively successful in these aspects, it is found that the p_T distribution of the lepton pairs is too broad to be accounted for by the small intrinsic transverse momentum of the two annihilating quarks, and the over-all cross-section is larger by a factor $K \approx 2$ than what is predicted within the $q\bar{q}$ annihilation mechanism [5-8]. These problems are being studied theoretically, and it appears that QCD corrections to the Drell-Yan mechanism could increase the cross-section by nearly a factor of 2 [9] and explain the large p_T released to the lepton pairs [10]. In pp interactions such as at the ISR, the so-called Compton diagram (gluon-quark scattering) is expected to dominate at large transverse momenta, and a quark jet should recoil against the lepton pair. Since no dynamical correlations are expected in the original Drell-Yan model, any such effect would be indicative of other dynamical mechanisms. These are precisely the problems probed by the present experiment.

The recoiling jet in our kinematic range would have small multiplicity and large opening angle, typically two to four charged particles with relative angles of the order of 20°, as at SPEAR/DORIS. Although it is difficult to isolate such a recoiling jet cleanly because of the physical background due to the fragments of the projectiles, which extends to small c.m. rapidities, and because of the limited p_T range available within the statistics of our experiment ($p_T \lesssim 5$ GeV/c), there are qualitative features that can be checked, such as whether anomalous clustering of particles exists in μ-pair events. If these clusters are due to the above-mentioned QCD effects, they should be emitted at opposite azimuth with respect to the μ pair, in stronger correlation than is enforced by momentum conservation. If the production mechanism involves a valence quark hitting a gluon (or a sea antiquark) which has a small longitudinal momentum, the cluster should also be produced closely in rapidity to the μ pair (positive cluster/μ-pair correlation). As will be shown in the following, there are similar effects in the data.

1. THE EXPERIMENT

The μ-pair detector is an assembly of trigger counters and planar drift chambers interspaced with magnetized iron toroids surrounding the ISR beam pipe, as shown in fig. 1. This detector covers angles $80° < \theta < 165°$ with respect to beam 1, and is described in detail in ref. 3. Immediately outside the pipe and within a rectangular volume 80 × 80 cm^2 in section, several telescopes of small drift chambers [11] determine three to five points for each charged particle emitted within $9° \lesssim \theta \lesssim 171°$ over the whole azimuth. The chambers have miniaturized frames and employ delay lines parallel to the sense wires, thus directly measuring space points for each charged track before entering the magnetized toroid spectrometers that filter the hadrons out and measure the muon momenta. Downstream of beam 1 and outside the toroid enclosure, two telescopes of planar drift chambers, also using delay lines [12], extend the coverage of the vertex detector to angles as small as 1°. An artist's view of the central detector and of the forward telescope is shown in fig. 2.

Muon trajectories were determined using the chambers between the toroids, and were extrapolated backwards to give a rough event vertex. The vertex detector was used to reconstruct an accurate event vertex using clear tracks in the vertex detector. The μ-pair momentum was finally obtained, making use of the reconstructed vertex as well as of the tracks in the outer chambers.

In the study of hadron correlations, a minimum $\int B\, d\ell$ of about 23 kG•m was requested for each muon of the pair. This cut played a role in reducing the background of hadron punch-through and decay, which was monitored by the rate of like-sign "μ pairs". The contamination was thus reduced to $\lesssim$ 40% of the signal for $m_{\mu\mu} < 4$ GeV, to $\lesssim$ 15% for $4 < m_{\mu\mu} < 6$ GeV, and to almost zero for $m_{\mu\mu} > 6$ GeV. The event sample was further reduced by requiring both muons leaving the detector to have double space points. No correction was applied in the analysis to account for such a background in the 1868 opposite-sign μ-pair events accepted by the cuts. These events were analysed by a refined reconstruction program to find all tracks, rescuing as far as possible all hits in the central chambers. Those tracks fitting the outer muon trajectories were excluded, and the remaining tracks were examined for correlations.

2. EFFICIENCY OF THE VERTEX DETECTOR

The efficiency of reconstructing a given particle track was determined to be 81%. This was done by Monte Carlo simulation of tracks with subsequent reconstruction imposing the criteria used in the analysis program. From the production mechanism we used, we estimate a systematic uncertainty of 5%. For dimuons as determined from the outside chambers, the measured and the calculated reconstruction efficiencies agreed well. As a consistent check of our detector we compare our raw multiplicity distribution with a minimum bias trigger, with published data at the same energy [13], as shown in fig. 3. We find $\langle n_{ch} \rangle = 10.2$ with dispersion $D = 5.8$, with an acceptance calculated by the Monte Carlo method to be 81%. With respect to ref. 13, both $\langle n_{ch} \rangle$ and D are smaller by $\sim$ 20%. This is precisely what would be predicted if there was a 20% probability of losing tracks in each event. We also find, by an inspection of the inclusive pseudorapidity distribution

of tracks, that there are zones of inefficiency which indeed amount to about 20%. Therefore, we conclude that our loss is of the order of 20%, with little dependence on the type of event. This situation is fully adequate for the study of correlations and of relative effects, which are the subject of this paper.

3. RESULTS

3.1 Associated multiplicities and angular distributions

We made an extensive search for the best variables to bring dynamical correlations into evidence. The dynamical variables available in the associated hadronic production with dimuons are the dimuon mass, the c.m. energy $\sqrt{s}$, and the longitudinal and transverse components of the dimuon momentum. Varying any of these variables can change the dynamics and the kinematics of the process, with corresponding variations in the hadron correlations. Since an appreciable fraction of the energy available for hadronization is usually carried away by the μ pair, and in order to minimize the kinematics effect due to the constraints of energy-momentum conservation, in analysing our data we use the invariant mass of the hadronic system, $M_h = (s + m_{\mu\mu}^2 - 2\sqrt{s}\, E_{\mu\mu})^{\frac{1}{2}}$, instead of using $m_{\mu\mu}$ and $\sqrt{s}$ separately. This variable reduces to the available energy for hadronization, $E_h = \sqrt{s} - E_{\mu\mu}$, when the dimuon energy $E_{\mu\mu}$ is much smaller than the c.m. energy $\sqrt{s}$.

We found that the main features of the associated hadron system no longer depend separately on the mass of the dimuon and on s, but only on M_h. There may be an exception to this rule when $m_{\mu\mu} < 4$ GeV (J events), as will be discussed in the following.

Figure 4 shows the total raw multiplicity as a function of M_h. For small energy carried away by the μ pair ($M_h \sim 60$ GeV), the charged multiplicity is $\langle n_{ch} \rangle \gtrsim 15$, which is larger by about 5 units than in inclusive events ($\langle n_{ch} \rangle \sim 10.2$ in our raw inclusive data). This shows that μ-pair events are always highly inelastic collisions. We see that the multiplicity increase with increasing M_h is much stronger than the dependence of $\langle n_{ch} \rangle$ on $\sqrt{s}$ for inclusive inelastic pp collisions [13], shown as a dash-dotted curve in the same figure. Without necessarily

invoking specific hard-scattering mechanisms between proton constituents to produce the μ pair, this effect can be qualitatively attributed to a faster energy dependence of $\langle n_{ch} \rangle$ on energy in highly inelastic events. The slope of the data -- approximately 0.3 particle per GeV -- extrapolates to $\langle n_{ch} \rangle \sim 0$ for $M_h \sim 0$, which indicates that there is no leading-particle effect in μ-pair events. It is thus natural to compare particle production in the μ-pair data with e^+e^- annihilation at $\sqrt{s} = M_h$. To do this, we have increased our raw multiplicity by 20% to account for the incomplete acceptance, as discussed in Section 2. The data are presented in fig. 5, in comparison with e^+e^- data up to $\sqrt{s} = 32$ GeV [14]. We observe that both the magnitude and the M_h dependence are in fair agreement with the trend of the e^+e^- data. Our data are also in good qualitative agreement with inclusive pp data once the leading protons have been removed [15]. Detailed comparison of rapidity distributions and short-range correlations, which could be indicative of the nature of the mechanism of particle production in the plateau region as well as in the fragmentation cones [16], will be the subject of our future work.

Figure 6 shows the same data split into low-p_T and high-p_T events for three intervals of dimuon mass. We see no significant difference between events of the same M_h and different $m_{\mu\mu}$ as anticipated earlier. On the other hand, the data at $p_T > 1.5$ GeV/c show consistently higher multiplicity than that at $p_T < 1.5$ GeV. Qualitatively it may be argued that for any M_h, hadronic systems recoiling against the μ pair with larger $p_T = -p_T^{\mu\mu}$ suffer a larger acceleration and are thus likely to materialize into a larger number of hadrons. According to QCD, if quark or gluon jets are present in large p_T events superimposed to normal production, the multiplicity is expected to be higher. Figure 6 indicates that $\langle n_{ch} \rangle$ depends basically only on M_h and p_T. To see this better, in fig. 7 we show the data as a function of M_h, for three bins of p_T up to $p_T = 5$ GeV/c. The best-fit straight lines have slopes that might be changing with p_T but cannot be distinguished within the errors: 0.40 ± 0.06 particle/GeV for $p_T < 1.5$ GeV/c, 0.31 ± 0.06 particle/GeV for $1.5 < p_T < 3$ GeV/c, and 0.17 ± 0.14 particle/GeV for $3 < p_T < 5$ GeV/c. The average multiplicities are $\langle n_{ch} \rangle = 13.7$, 14.1, and 14.3 for $p_T < 1.5$, $1.5 < p_T < 3$, and $3 < p_T < 5$ GeV/c, respectively.

The multiplicity in the two hemispheres towards and away from the transverse momentum of the μ pair behave very differently as a function of p_T, as shown in fig. 8. The away multiplicity grows with p_T while the towards multiplicity decreases slightly, which can be easily understood as a reflection of a decreasing M_h with increasing p_T. As a rough approximation we can take the p_T and M_h dependences to factorize and summarize our raw data by saying that ≈ 0.3 particle is produced per GeV of available hadronic energy, and in addition ≈ 0.6 particle is produced in the away hemisphere per GeV/c of transverse momentum. The p_T dependence of the away multiplicity is similar at any M_h, the main difference being the absolute value of the associated multiplicity. This is seen in fig. 9, where $\langle n_{ch,away} \rangle$ is plotted versus p_T for three intervals of M_h. We note that the dependence of $\langle n_{ch,away} \rangle$ on p_T is very similar to what was previously found for large p_T π^0 events [17].

The azimuthal distribution of tracks from 0° to 180°, relative to the $\vec{p}_T$ of the dimuon in the c.m.s. frame, is shown in fig. 10 for two intervals of hadronic energy: $M_h > 56$ GeV ($\langle M_h \rangle \sim 58$ GeV) and $M_h < 56$ GeV ($\langle M_h \rangle \sim 52$ GeV). In order to minimize contamination of tracks originated by the incident proton fragmentation, tracks at $\theta < 39°$ relative to each beam (fragmentation cones) have been excluded. For the two M_h ranges, the distributions are studied for four p_T bins. For the $M_h > 56$ GeV, because of phase-space constraints one selects mostly J events. The data are almost independent of p_T, with the asymmetry ε defined as (away-towards)/towards fitted to be $\varepsilon = (-4 \pm 4)\%$ at $0 < p_T < 1$ GeV/c, $\varepsilon = (9 \pm 3)\%$ at $1.0 < p_T < 2.0$ GeV/c, $\varepsilon = (14 \pm 8)\%$ at $2.0 < p_T < 4.0$ GeV/c, and $\varepsilon = (27 \pm 43)\%$ at $4 < p_T < 6$ GeV/c. On the other hand, in the $M_h < 56$ GeV sample the backward excess of particles increases quickly with p_T. We find $\varepsilon = (-4 \pm 6)\%$ for $0 < p_T <$ < 1.0 GeV/c, $\varepsilon = (27 \pm 6)\%$ for $1.0 < p_T < 2.0$ GeV/c, $\varepsilon = (30 \pm 7)\%$ for $2.0 < p_t <$ < 4.0 GeV/c, and $\varepsilon = (54 \pm 16)\%$ for $4 < p_T < 6$ GeV/c. The difference between the correlations in the two M_h intervals may be dynamical in origin. For the $M_h >$ > 56 GeV events, since the away multiplicity in this M_h sample is increasing with p_T and ε is small, it can be concluded that a flat azimuthal distribution implies an equivalent increase of the toward multiplicity. Although the statistical

errors are large, this effect may be significant, and work is in progress for further investigation.

The average pseudorapidity $\langle\eta_{ch}\rangle$ ($\eta = -\ln \tan \theta/2$) of charged hadrons at $|\theta| > 39°$ was also studied as a function of the rapidity of the dimuon $y_{\mu\mu}$. When $y_{\mu\mu}$ varies from -0.25 to +1.0, $\langle n_{ch}\rangle$ also grows, with a small slope $\Delta\langle\eta_{ch}\rangle/\Delta y_{\mu\mu} \approx \approx (6 \pm 2)\%$. (See later, fig. 14.) This is suggestive of a small bunch of particles having a short-range positive correlation with the dimuon, superimposed onto normal uncorrelated production. We have studied such a possible effect in more detail, as explained in the following section.

3.2 Jet search

The general features of the associated production presented so far show that the hadronic correlations with the μ pair are similar to those already observed in large p_T π^0 production [17]. To interpret this data, it can be assumed that in each event some subsample of the hadronic system -- say a small jet or cluster of hadrons -- is more strictly correlated in rapidity (as well as in p_T) to the μ pair. In order to study such a possible effect, we have defined a leading hadronic cluster in each event as being that subsample of two or three hadrons possessing the maximum "thrust". The method employed was similar to that adopted in ref. 18. All the combinations of two or three tracks were considered in each event, and the one having the maximum $\sum_i^{2,3} \cos \theta_T^i$ was retained. To define this quantity, the axis relative to which the polar angle θ_T^i is measured was varied, and the thrust axis obtained was the one providing the maximum $\sum_i^{2,3} \cos \theta_T^i$. The event was labelled according to the average $\cos \theta_T^i$ (of the two or three tracks) in the selected cluster:

$$T = \langle \cos \theta_T^i \rangle \text{ in the cluster having maximum } \sum_i^{2,3} \cos \theta_T^i \ .$$

This method generates values of T that grow smoothly, for statistical reasons, with the event multiplicity as seen in fig. 11 both for μ-pair events and for inclusive events. Again in order to exclude clustering due to beam jets, tracks

at $\theta < 39^\circ$ relative to each beam have been excluded. The search for the narrowest cluster has been performed in two options, either including tracks at all azimuths (fig. 11a) or for tracks in the away hemisphere only (fig. 11b). We observe a very similar picture in these two cases and also an impressive similarity of clustering in μ-pair events and in inclusive events.

The azimuthal distribution of the T-axis for two intervals of hadronic energy is plotted in fig. 12. One sees an increasing backward peaking with increasing p_T in the $M_h < 56$ GeV data, but not in the $M_h > 56$ GeV data, representing the same features already apparent in fig. 10 in a neater and more consistent way. The effects are further enhanced if one selects only large T ($T > 0.85$) events as seen in fig. 13.

In order to study longitudinal correlations the average pseudorapidity of the T-axis $\langle\eta_T\rangle$ was studied as a function of the dimuon rapidity $y_{\mu\mu}$. These data are shown in fig. 14 (full points) for clusters at any M_h (no significant difference was found in longitudinal correlation for $M_h > 56$ GeV and $M_h < 56$ GeV). One observes a positive correlation $\Delta\langle\eta_T\rangle/\Delta y_{\mu\mu}$ of about $(11 \pm 5)\%$ in the interval $-0.25 < y_{\mu\mu} < 1$, consistent with the observed positive correlation $(6 \pm 2)\%$ for single tracks (open points in fig. 12) within statistics. These data are compared with the predictions of Monte Carlo generated events, in which three effects were superimposed: a) two fragmenting beam jets; b) a flat rapidity plateau at large angles; and c) a small jet of average multiplicity 3, emitted at 180° in azimuth relative to the μ pair with a Gaussian distribution with width $\pm\pi/4$, and at the same rapidity as the μ pair with a Gaussian distribution with width ±1. The parameters of the program were adjusted in order to fit the inclusive pseudorapidity distribution. The broken curve in fig. 14 represents the correlation of the thrust axis predicted by the Monte Carlo calculation. It can be seen that the Monte Carlo results agree qualitatively with the data. At large $y_{\mu\mu}$ a drop in correlation is caused by the cut at $\theta \geq 39^\circ$ which was imposed on single tracks.

The qualitative agreement between the data and the model shows that a mechanism involving associated production of a μ pair and of a small hadron jet, at approximately the same rapidity and emitted back-to-back in azimuth, would be consistent with our observation.

4. CONCLUSIONS

Our results can be summarized as follows. The hadronic production associated with μ pairs is much more abundant than in inclusive events, even at small $m_{\mu\mu}$ and small p_T. This indicates that the μ-pair events are highly inelastic, without much excess of energy released to the leading particles in the final state. The dependence of the associated multiplicity on the available energy M_h fits well with the trend indicated by the hadronic production in high-energy e^+e^- annihilation and with the charged multiplicity measured in inclusive pp collisions after correcting for the energy carried away by the leading particles.

The dependence of $\langle n_{ch} \rangle$ on p_T is similar to that observed in other large p_T events, with the multiplicity in the away hemisphere increasing rapidly with p_T. Small clusters appear to be produced at large angles in μ-pair events as well as in inclusive events. In μ-pair events the correlation, both in azimuth and in rapidity, of the narrowest of these clusters with the μ pair can be reproduced with a simple Monte Carlo model in which a cluster of few particles produced locally in rapidity and backwards in azimuth with respect to the μ pair, is superimposed onto a normal event.

Acknowledgements

Prof. Samuel C.C. Ting had a leading role in the inclusive μ-pair production experiment. We also thank Prof. K. Strauch for his contribution during the initial phase of the experiment. We gratefully acknowledge the continuous support extended to the Group by the CERN Directorate. The staff of the Intersecting Storage Rings Division, and especially the ISR Experimental Support Group, have been extremely helpful. The excellent engineering of the central detector is due to F. Bosi and G. Ciancaglini. The dedication and skill of our group of technicians, A. Bechini, C. Betti, U. Cazzola, M. Favati, F. Manna, P. Marchi and V. Marzullo, were essential for the successful operation of the hadron detector.

REFERENCES

[1] J.J. Aubert et al., Phys. Rev. Lett. 33 (1974) 1404.

[2] S.W. Herb et al., Phys. Rev. Lett. 39 (1977) 252.

[3] D. Antreasyan et al., Phys. Rev. Lett. 45 (1980) 863.

[4] S.D. Drell and T.M. Yan, Phys. Rev. Lett. 25 (1970) 316, 920(E).

[5] D. Antreasyan et al., Phys. Rev. Lett. 47 (1981) 12.

[6] C.B. Newman et al., Phys. Rev. Lett. 42 (1979) 951.
L. Lederman, Proc. 19th Int. Conf. on High-Energy Physics, Tokyo, 1978 (Physical Society of Japan, Tokyo, 1979), p. 706.
R. Kienzle, Proc. Int. Symposium on Lepton and Photon Interactions at High Energy, Batavia, 1979 (Fermilab, Batavia, 1980), p. 161.
M.J. Corden et al., preprint CERN-EP/80-152 (1980).

[7] J.E. Pilcher, Proc. Int. Symposium on Lepton and Photon Interactions at High Energy, Batavia, 1979 (Fermilab, Batavia, 1980), p. 185.

[8] J. Badier et al., Phys. Lett. 89B (1979) 145 and preprint CERN-EP/80-147 (1980).

[9] G. Altarelli, R.K. Ellis and G. Martinelli, Nucl. Phys. B157 (1979) 461.
J. Kubar and F.E. Paige, Phys. Rev. D 19 (1979) 221.

[10] For a discussion on possible mechanisms leading to large p_T of lepton pairs, see for instance E.L. Berger, Hadroproduction of massive lepton pairs and QCD, Stanford preprint SLAC-PUB-2234 (1979).

[11] A. Bechini et al., Nucl. Instrum. Methods 156 (1978) 181.

[12] F. Carbonara et al., Nucl. Instrum. Methods 171 (1980) 479.

[13] W. Thomé et al., Nucl. Phys. B129 (1977) 365.

[14] The e^+e^- data can be found in PLUTO Collaboration, Ch. Berger et al., Phys. Letters 95B (1980) 313.

[15] M. Basile et al., Phys. Lett. 95B (1980) 311.

[16] J. Ellis, private communication.

[17] R. Kephart et al., Phys. Rev. D 14 (1976) 2909.

[18] DASP II, presented by W. Schmidt-Parzefall, *in* Proc. Int. Conf. on High-Energy Physics, Tokyo, 1978 (Physical Society of Japan, Tokyo, 1979), p. 260.

Figure captions

Fig. 1 : General layout of the experiment.

Fig. 2 : Layout of the vertex detector: forward telescope (top) and central detector (bottom).

Fig. 3 : Raw multiplicity distribution of charged tracks in minimum bias events at $\sqrt{s}$ = 62 GeV, compared with the measurement reported in ref. 13. The data have been collected with an inclusive trigger in between μ-pair runs, i.e. at high luminosity and large source dimension. Our data have $\langle n_{ch} \rangle = 10.2$ with D = 5.8, while the data of ref. 13 have $\langle n_{ch} \rangle = 12.7$ with D = 6.9.

Fig. 4 : Raw associated multiplicity in μ-pair events as a function of the invariant mass of the final-state hadronic system. The data extrapolate to $\sim$ 5 particles more than in unbiased inelastic events at $M_h = \sqrt{s} = 62$ GeV, and to $\langle n_{ch} \rangle \sim 0$ at $M_h = 0$ (the slope being 0.28 ± 0.4 particle/GeV). The dash-dotted curve represents a fit to the pp inclusive multiplicity [13].

Fig. 5 : Comparison between multiplicities measured in e^+e^- annihilation and multiplicities associated with μ pairs at $M_h = \sqrt{s}$. The broken curve is a logarithmic fit to e^+e^- low-energy data. ISR data with the energy of leading particles removed are also shown [15]. The full curve is a fit to the large ($10 < \sqrt{s} < 32$ GeV) energy e^+e^- data [14]. The dash-dotted curve is a fit to the pp inclusive multiplicity [13].

Dependence of multiplicity on M_h for low ($p_T < 1.5$ GeV/c) and high ($p_T > 1.5$ GeV/c) transverse momenta of the μ pair.

$\langle n_{ch} \rangle$ versus M_h, for three intervals of p_T. All μ-pair masses were included. Relevant parameters are (from small to large p_T):
• = $\langle n_{ch} \rangle = 13.7 \pm 0.2$, $\langle p_T \rangle = (0.93 \pm 0.01)$ GeV/c, slope = 0.40 ± 0.06 particle per GeV/c; o: $\langle n_{ch} \rangle = 14.1 \pm 0.3$, $\langle p_T \rangle = 2.05 \pm 0.02$ GeV/c, slope = 0.31 ± 0.06 particles per GeV/c; *: $\langle n_{ch} \rangle = 14.3 \pm 0.6$, $\langle p_T \rangle = 3.67 \pm 0.04$ GeV/c, slope = 0.17 ± 0.14 particle per GeV/c.

Fig. 8 : $\langle n_{ch} \rangle$ versus p_T, in the hemispheres towards and away from the transverse momentum of the μ pair. The fitted curve to the away data (first 7 points) has a slope of 0.6 ± 0.2 particle per GeV/c.

Fig. 9 : $\langle n_{ch} \rangle$ in the away hemisphere versus p_T. All μ-pair masses were included. The slopes of the fitted straight lines to the data are: •: 0.6 ± 0.2 particle per GeV/c; o: 0.6 ± 0.06 particle per GeV/c; *: 0.7 ± 0.3 particle per GeV/c.

Fig. 10 : Azimuthal distribution of tracks at $|\theta| > 39°$ relative to the μ pair transverse momentum, for two ranges of hadronic energy corresponding to $\langle M_h \rangle \approx 52$ GeV and $\langle M_h \rangle \approx 58$ GeV. The distributions are given for four intervals of p_T. ε is the excess in the away hemisphere relative to the toward one.

Fig. 11 : Dependence of the average thrust of the associated narrowest hadron clusters (see text for details) on event multiplicity over the full solid angle (a) or in the away hemisphere only (b). The data are presented for μ-pair events and for minimum bias events.

Fig. 12 : Azimuthal distribution of the thrust axis for $M_h > 56$ GeV (mostly J events) and $M_h < 56$ GeV, for three intervals of p_T.

Fig. 13 : Same as fig. 12 but $T > 0.85$.

Fig. 14 : Average pseudorapidity of the T-axis $\langle \eta_T \rangle$ as a function of the rapidity of the μ pair $y_{\mu\mu}$ (full points). The open circles show the average charged pseudorapidity $\langle \eta_{ch} \rangle$ as a function of $y_{\mu\mu}$. The data are compared with correlation of the T-axis predicted by the Monte Carlo calculation (broken curve, see text).

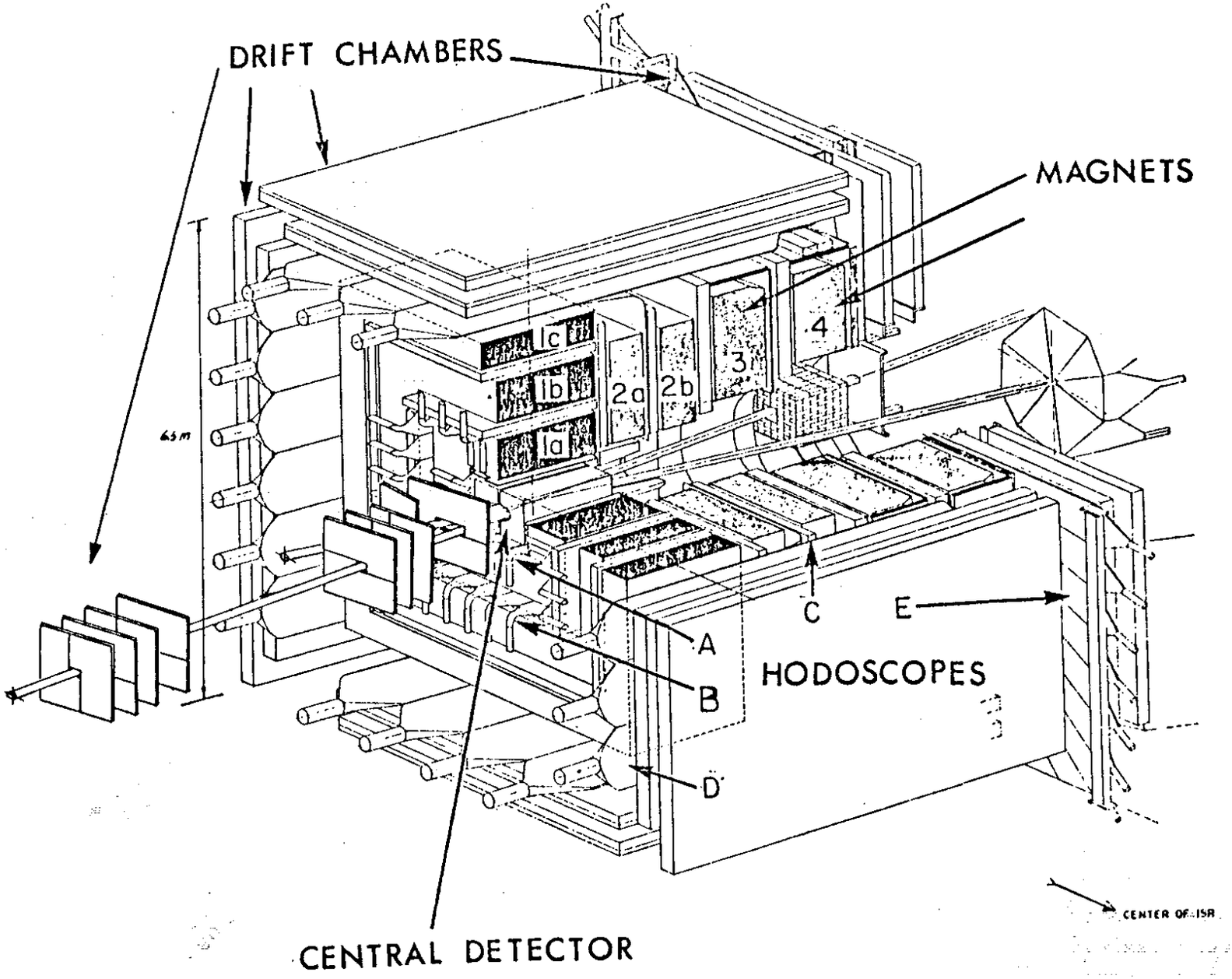
DRIFT CHAMBERS
MAGNETS
4.5 m
1c
1b
1a
2a
2b
3
4
A
B
C
D
E
HODOSCOPES
CENTRAL DETECTOR
CENTER OF ISR

Fig. 1

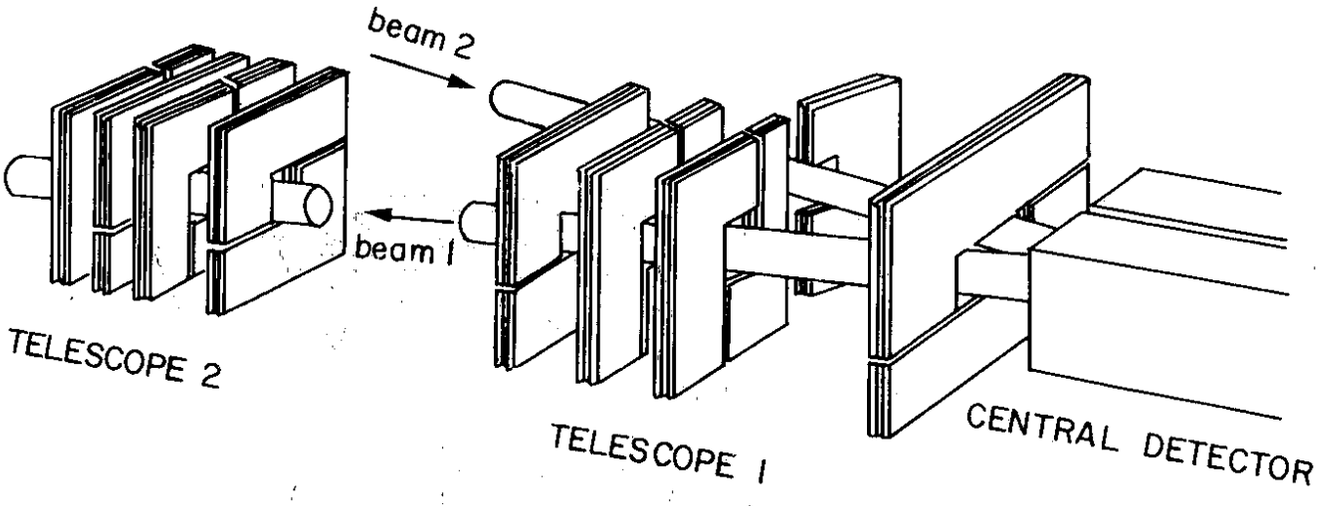
beam 2
beam 1
TELESCOPE 2
TELESCOPE 1
CENTRAL DETECTOR

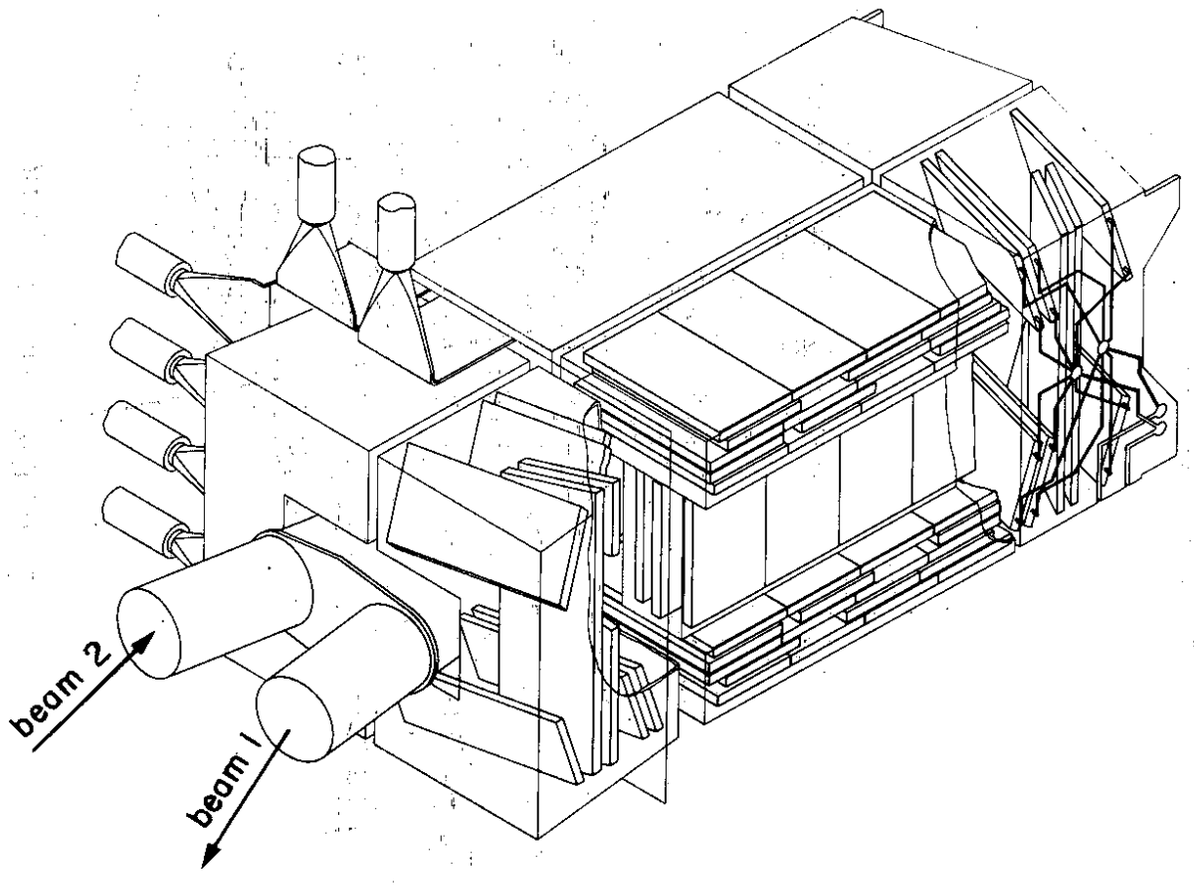
beam 2
beam 1

Fig. 2

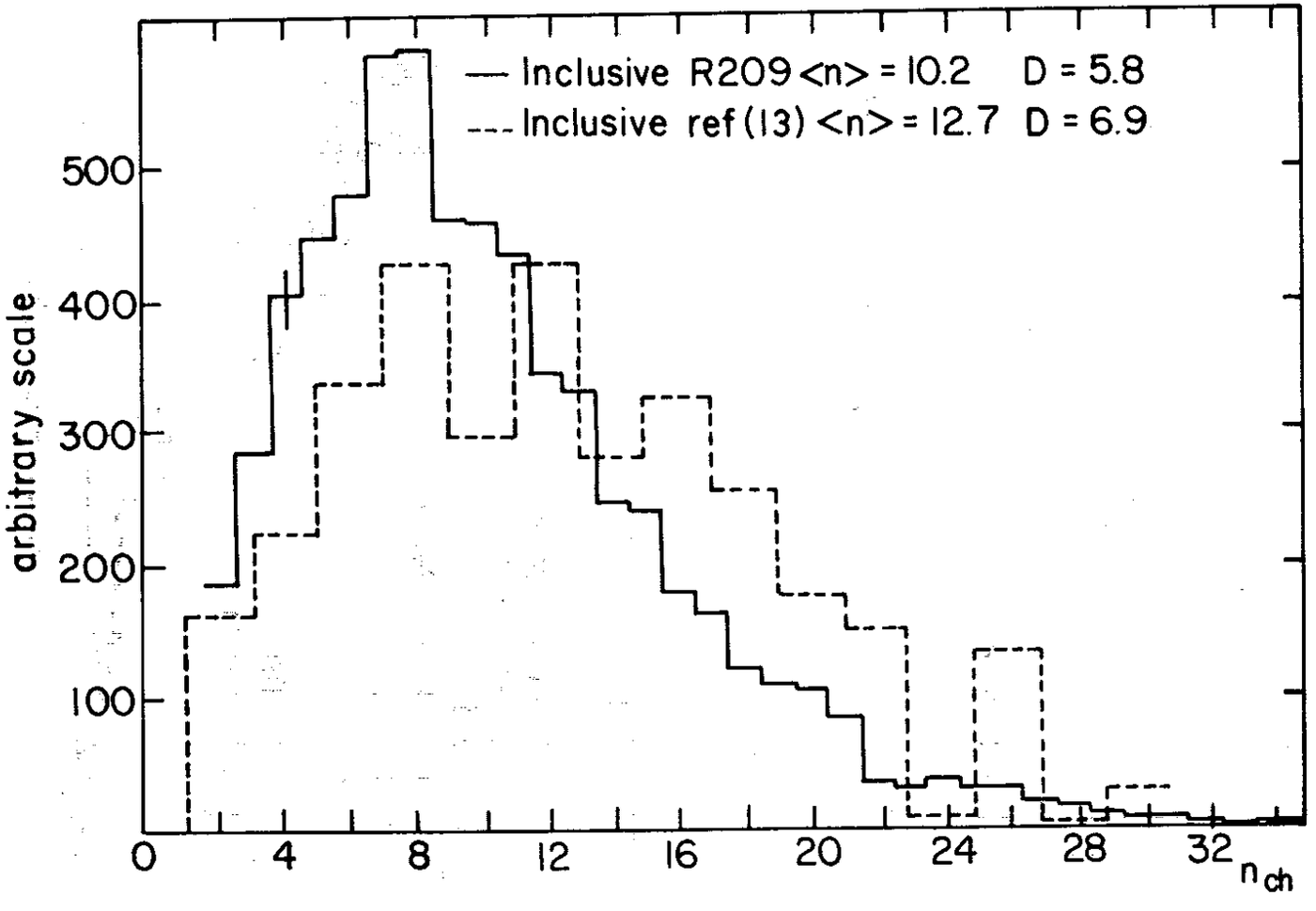
— Inclusive R209 <n> = 10.2 D = 5.8
--- Inclusive ref (13) <n> = 12.7 D = 6.9
arbitrary scale
500
400
300
200
100
0
4
8
12
16
20
24
28
32
n_{ch}

Fig. 3

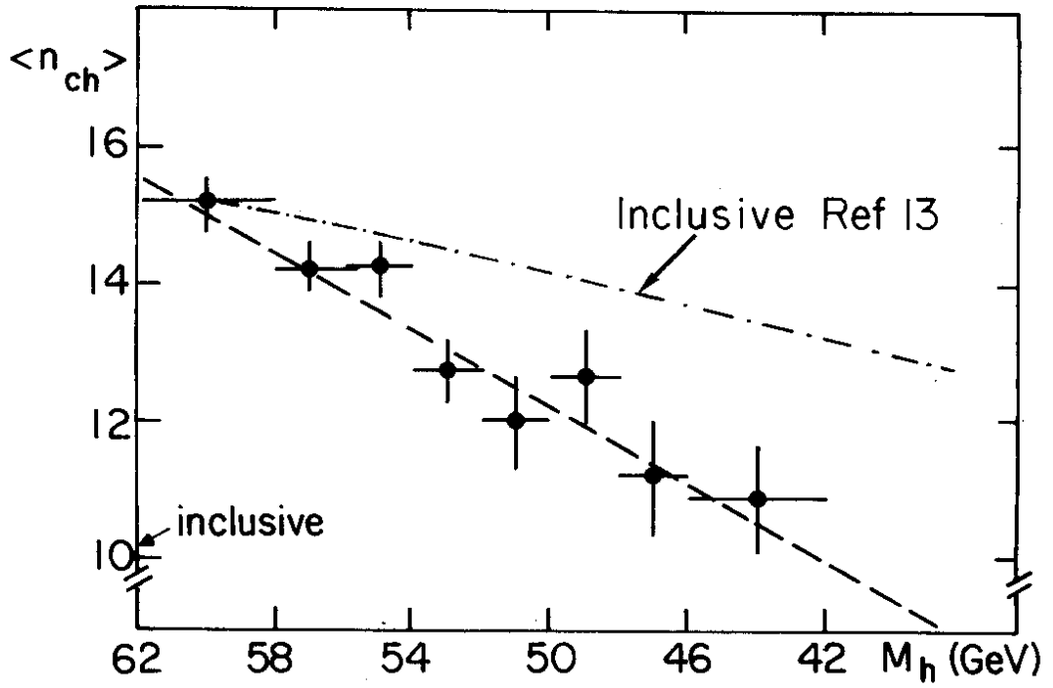
<n ch>
16
14
12
10
Inclusive Ref 13
inclusive
62
58
54
50
46
42
M h (GeV)

Fig. 4

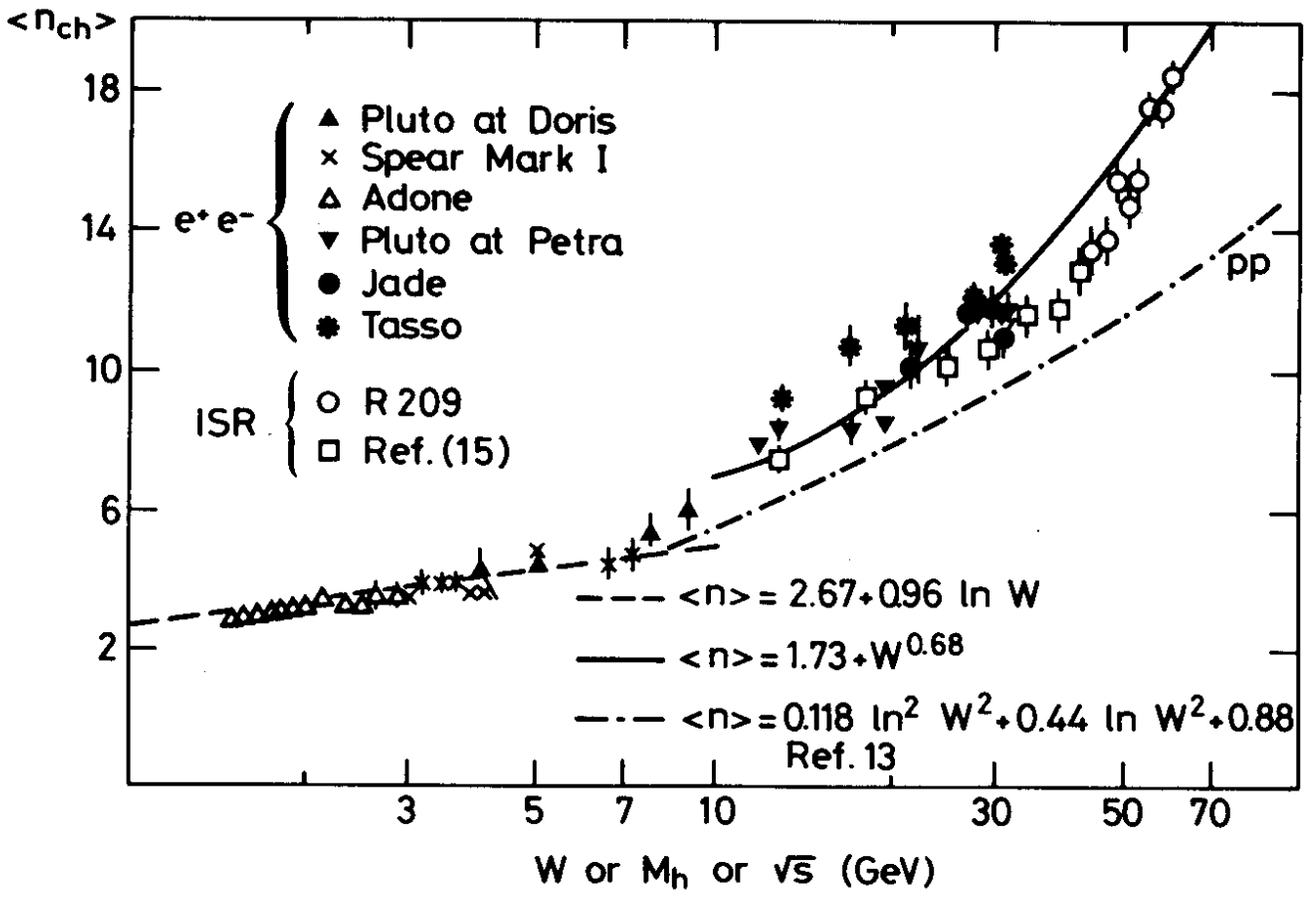
<n ch>
18
14
10
6
2
e+ e-
Pluto at Doris
Spear Mark I
Adone
Pluto at Petra
Jade
Tasso
ISR
R 209
Ref. (15)
pp
<n> = 2.67+0.96 ln W
<n> = 1.73+W^0.68
<n> = 0.118 ln^2 W^2+0.44 ln W^2+0.88
Ref. 13
3
5
7
10
30
50
70
W or M h or √s (GeV)

Fig. 5

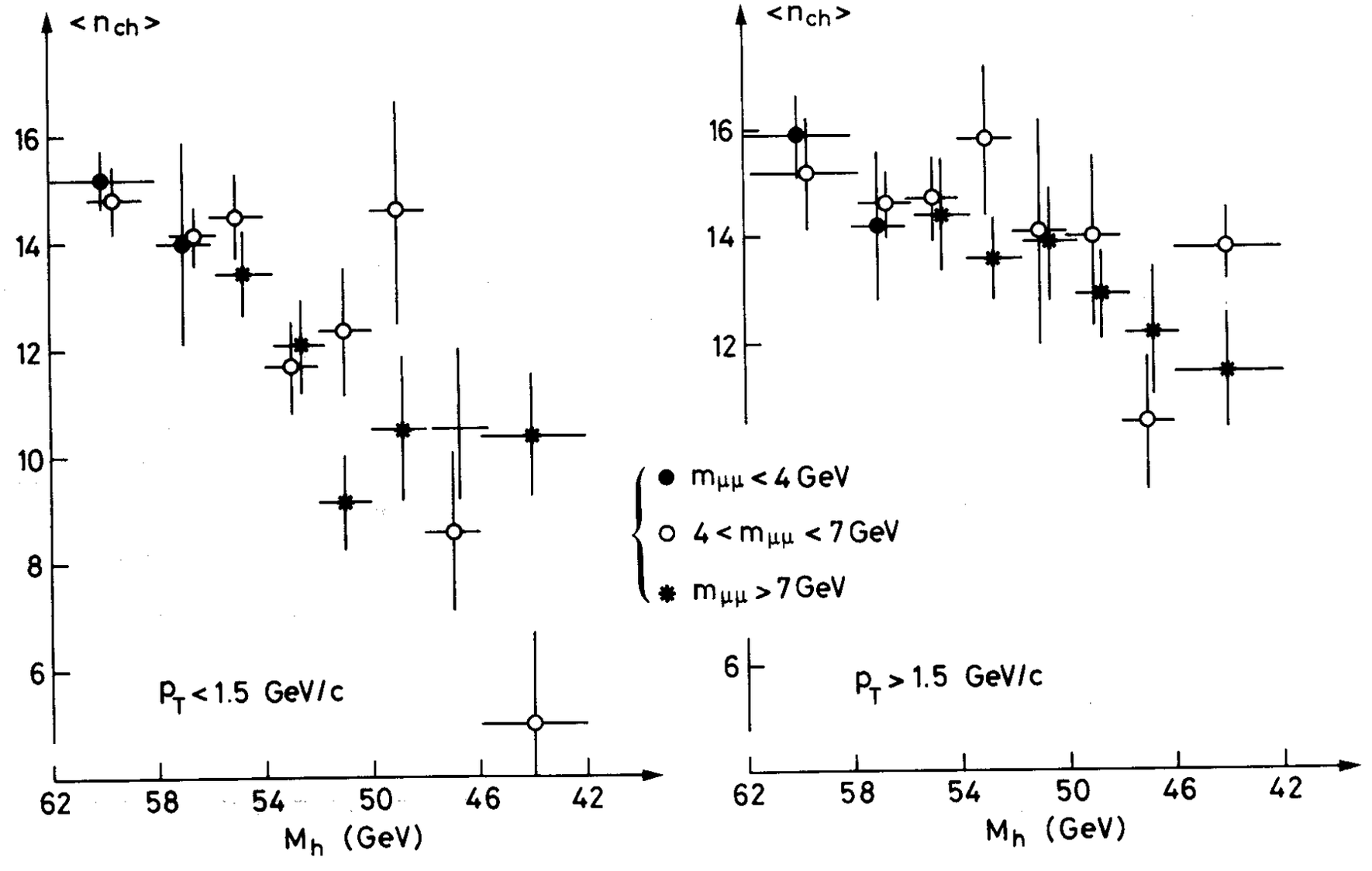
<n_ch>
16
14
12
10
8
6
62
58
54
50
46
42
M_h (GeV)
P_T < 1.5 GeV/c
<n_ch>
16
14
12
6
62
58
54
50
46
42
M_h (GeV)
P_T > 1.5 GeV/c
m_μμ < 4 GeV
4 < m_μμ < 7 GeV
m_μμ > 7 GeV

Fig. 6

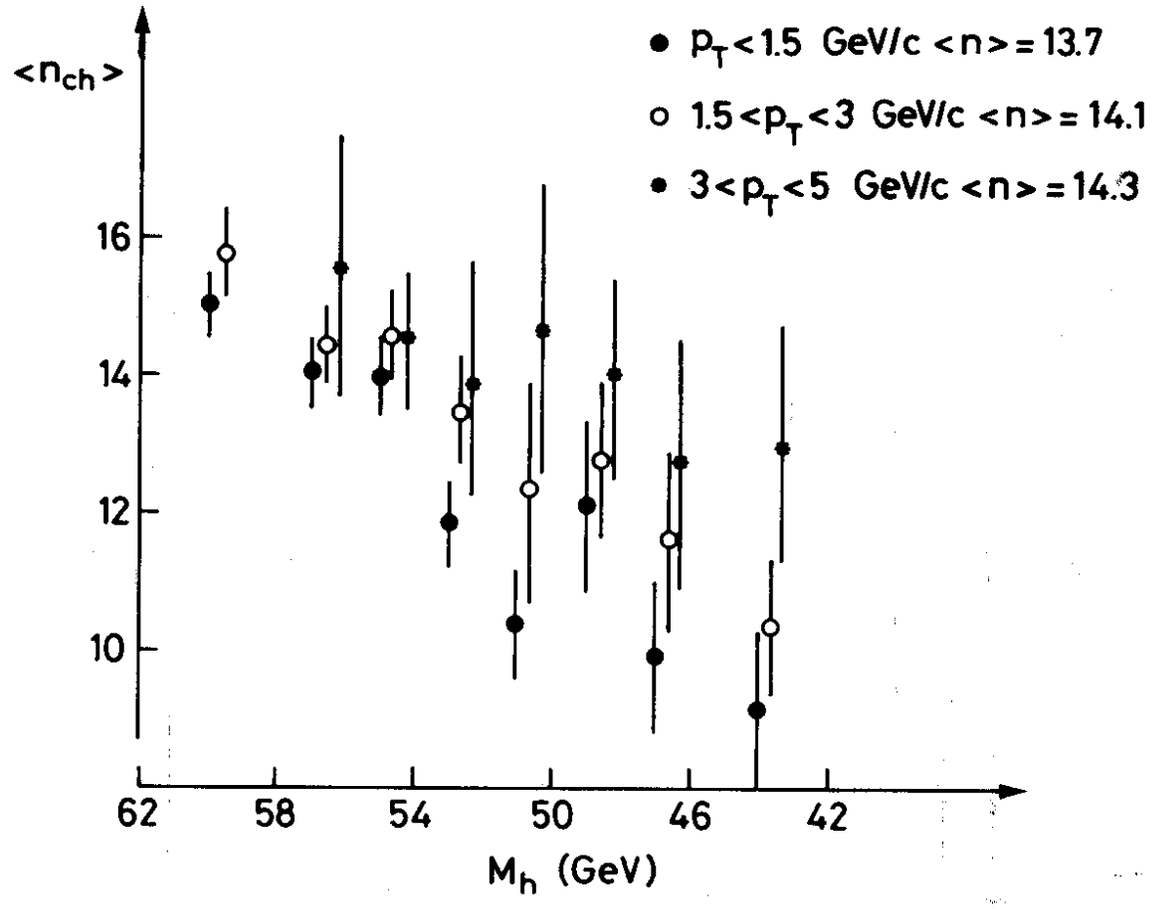
$\langle n_{ch} \rangle$
● $p_T < 1.5$ GeV/c $\langle n \rangle = 13.7$
○ $1.5 < p_T < 3$ GeV/c $\langle n \rangle = 14.1$
● $3 < p_T < 5$ GeV/c $\langle n \rangle = 14.3$
16
14
12
10
62
58
54
50
46
42
M_h (GeV)

Fig. 7

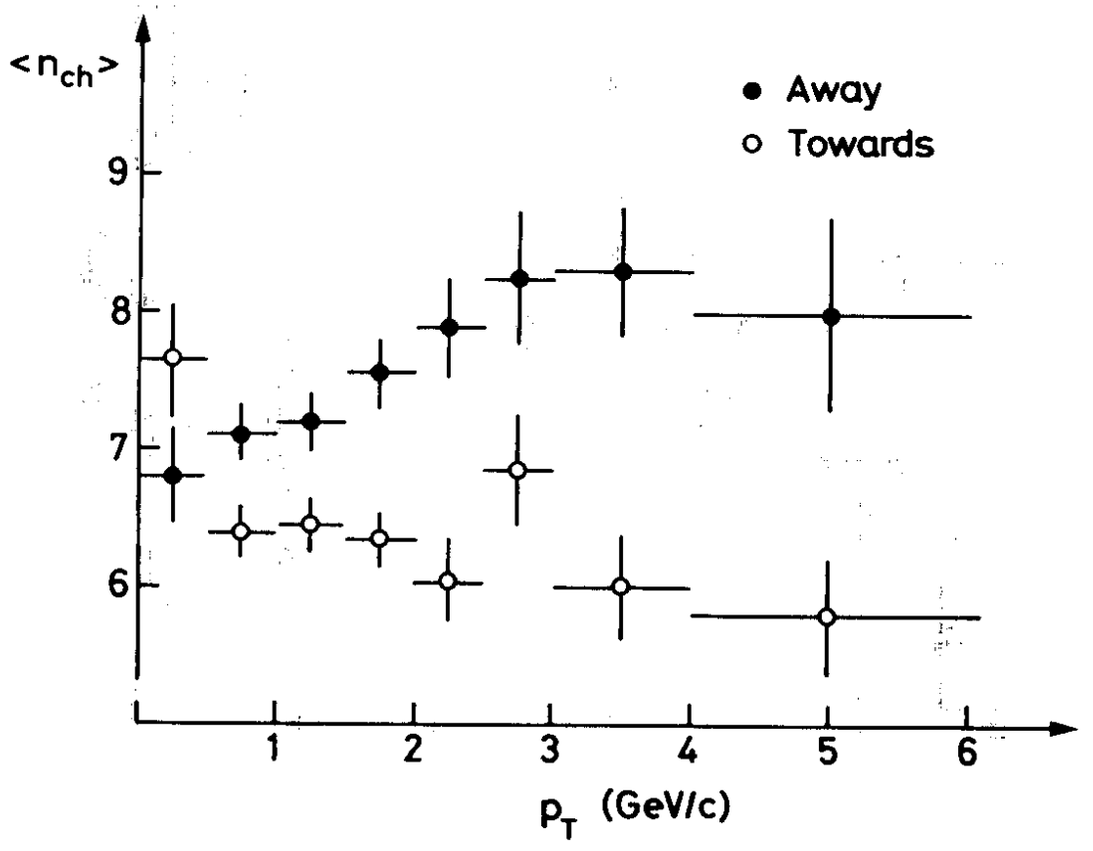
$\langle n_{ch} \rangle$
● Away
○ Towards
9
8
7
6
1
2
3
4
5
6
p_T (GeV/c)

Fig. 8

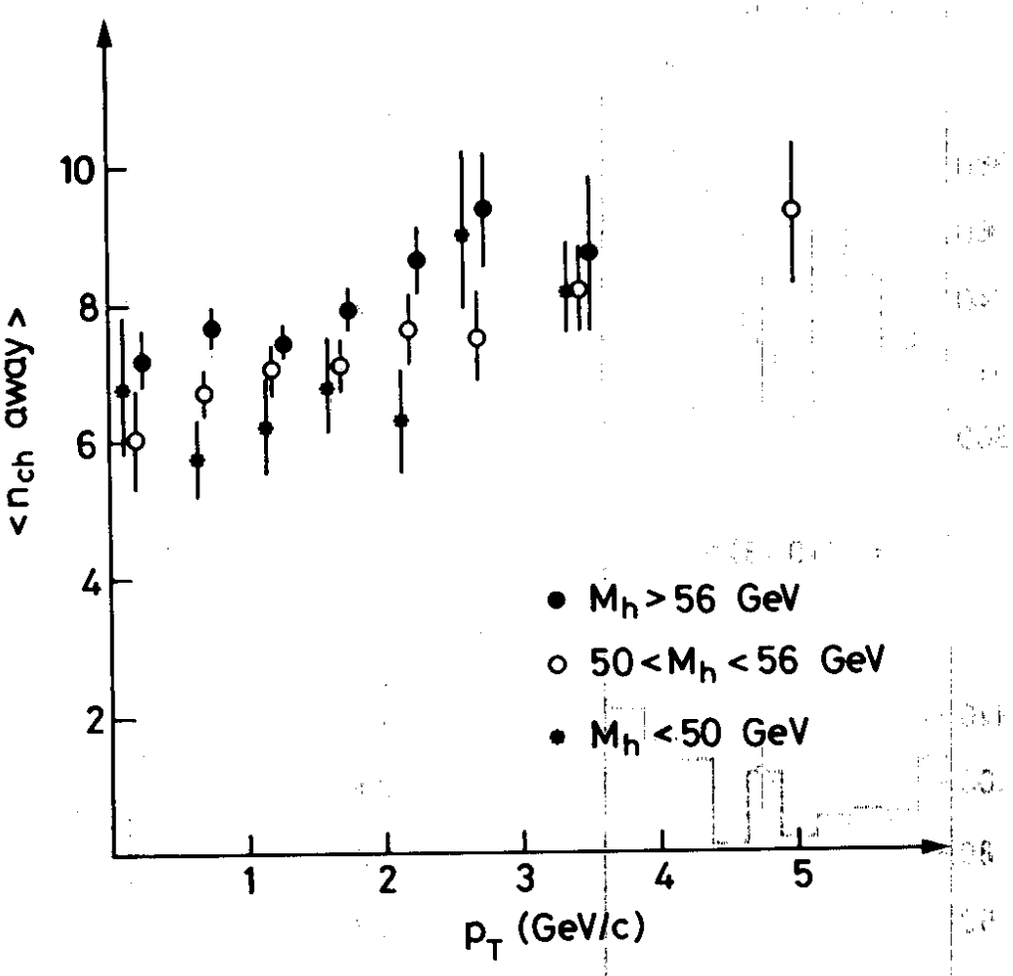
10
8
6
4
2
$\langle n_{ch}$ away $\rangle$
1
2
3
4
5
p_T (GeV/c)
● $M_h > 56$ GeV
○ $50 < M_h < 56$ GeV
• $M_h < 50$ GeV

Fig. 9

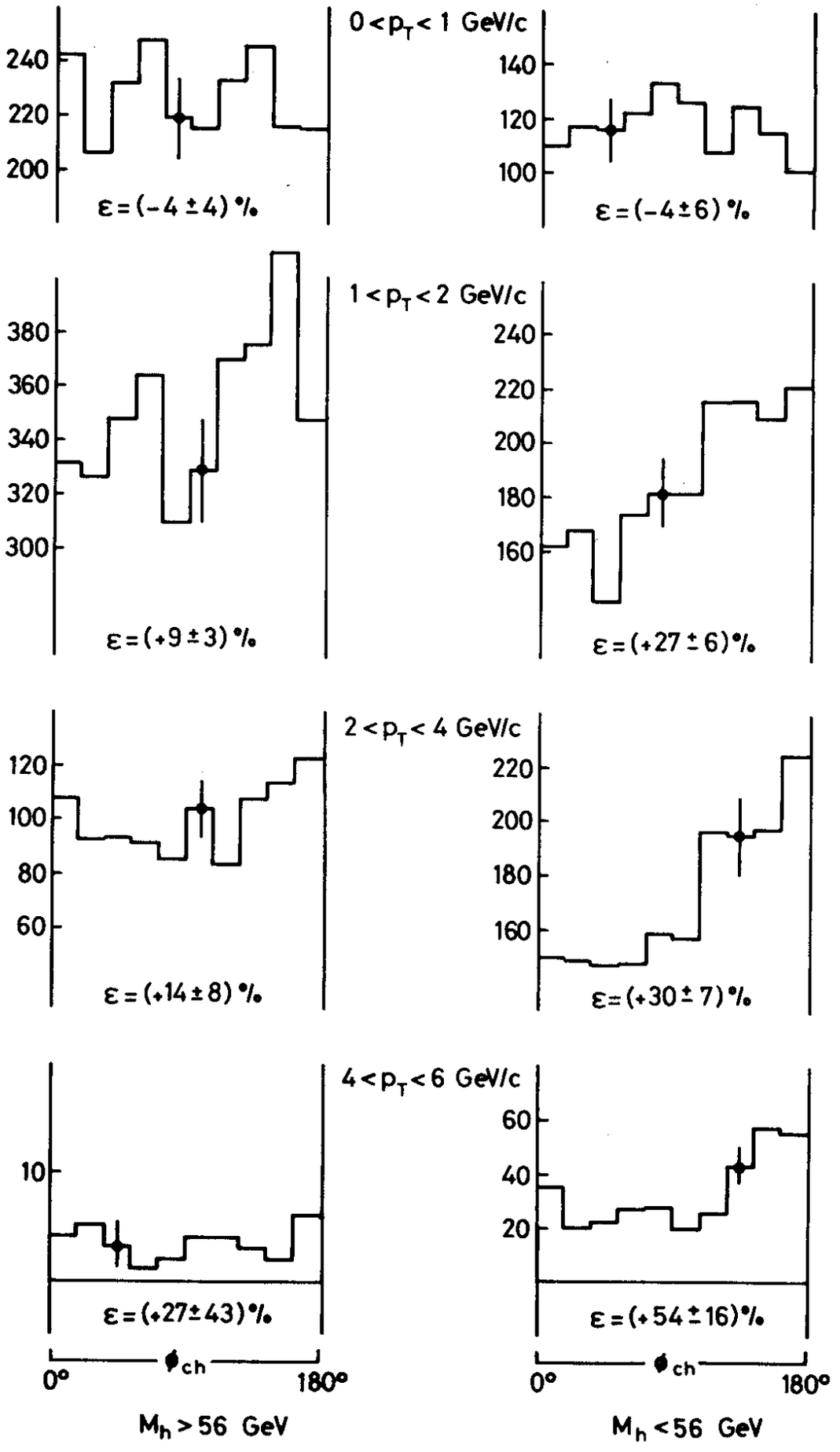
0 < p_T < 1 GeV/c
240
220
200
ε = (−4 ± 4) %
140
120
100
ε = (−4 ± 6) %
1 < p_T < 2 GeV/c
380
360
340
320
300
ε = (+9 ± 3) %
240
220
200
180
160
ε = (+27 ± 6) %
2 < p_T < 4 GeV/c
120
100
80
60
ε = (+14 ± 8) %
220
200
180
160
ε = (+30 ± 7) %
4 < p_T < 6 GeV/c
10
ε = (+27 ± 43) %
60
40
20
ε = (+54 ± 16) %
0°
ϕ_{ch}
180°
M_h > 56 GeV
0°
ϕ_{ch}
180°
M_h < 56 GeV

Fig. 10

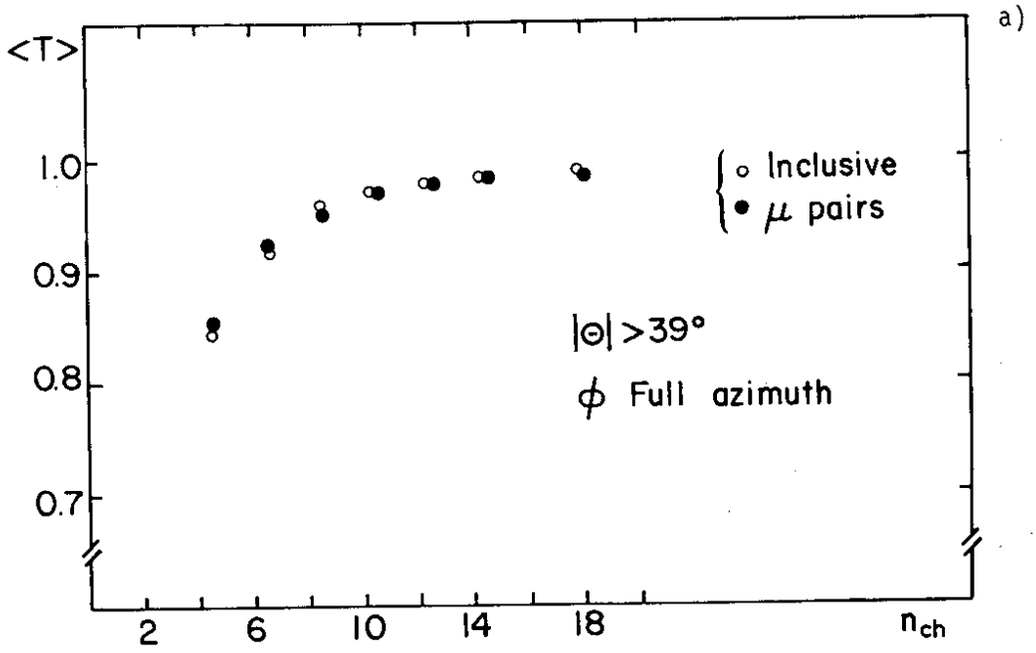
a)
<T>
1.0
0.9
0.8
0.7
2
6
10
14
18
n_{ch}
○ Inclusive
● μ pairs
|Θ| >39°
φ Full azimuth

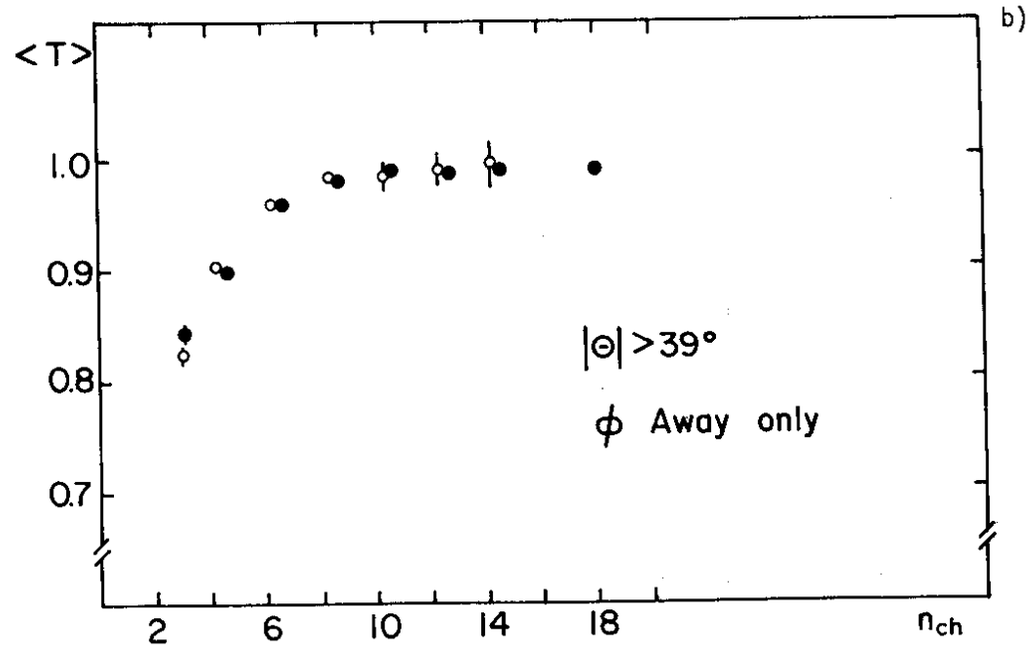
b)
<T>
1.0
0.9
0.8
0.7
2
6
10
14
18
n_{ch}
|Θ| >39°
φ Away only

Fig. 11

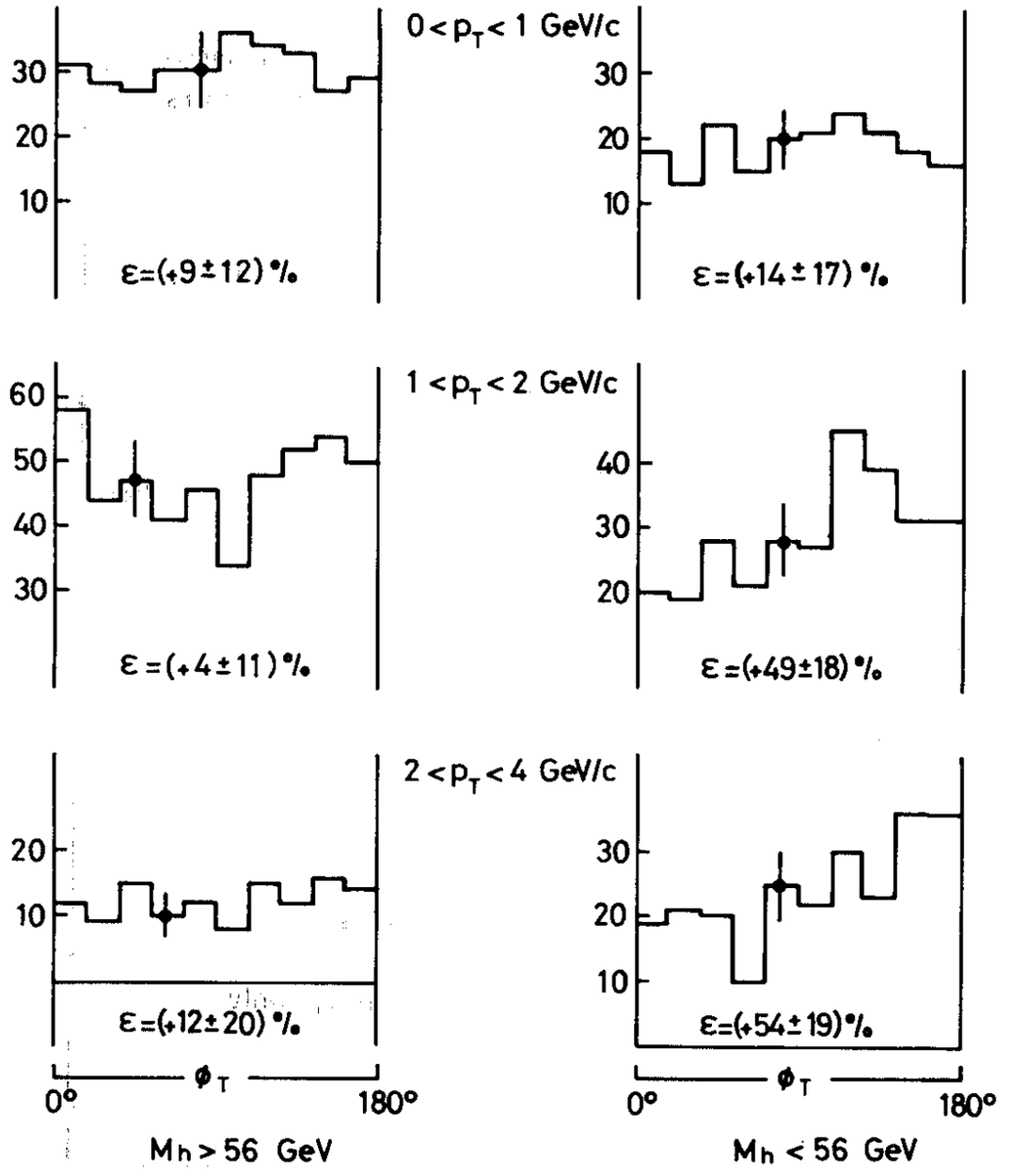
0 < pT < 1 GeV/c
1 < pT < 2 GeV/c
2 < pT < 4 GeV/c
ε=(+9±12) %
ε=(+14±17) %
ε=(+4±11) %
ε=(+49±18) %
ε=(+12±20) %
ε=(+54±19) %
φT
0°
180°
Mh > 56 GeV
Mh < 56 GeV

Fig. 12

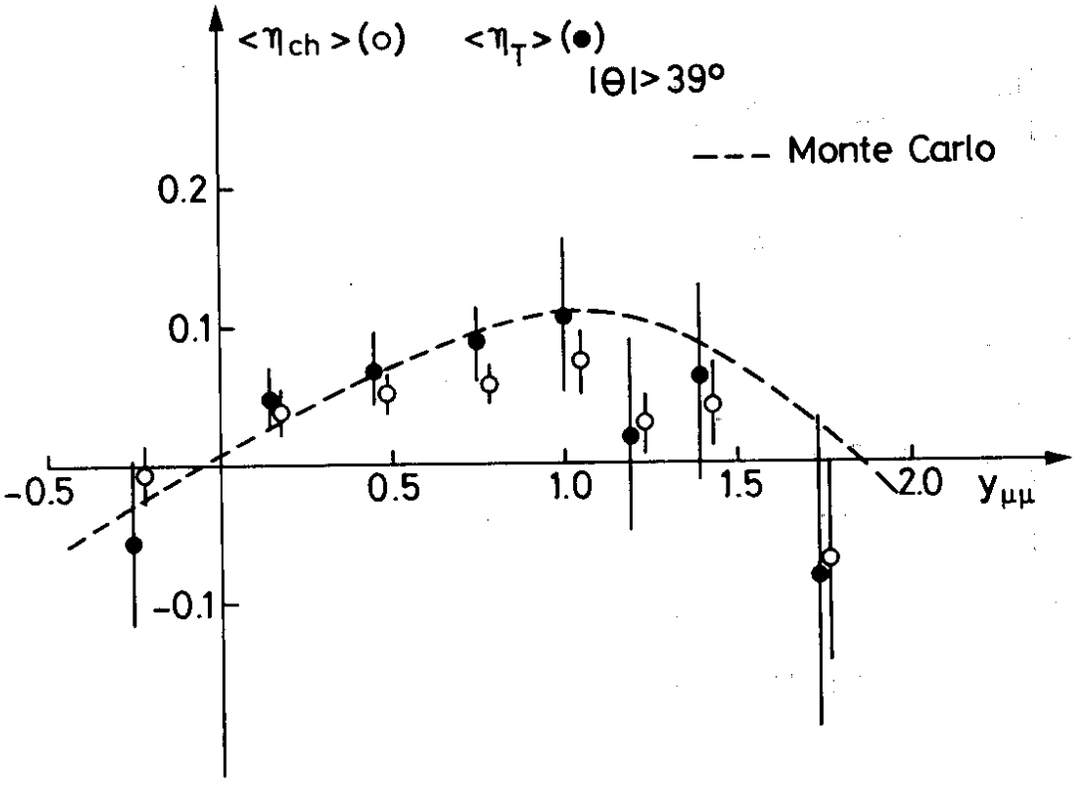

Fig. 14

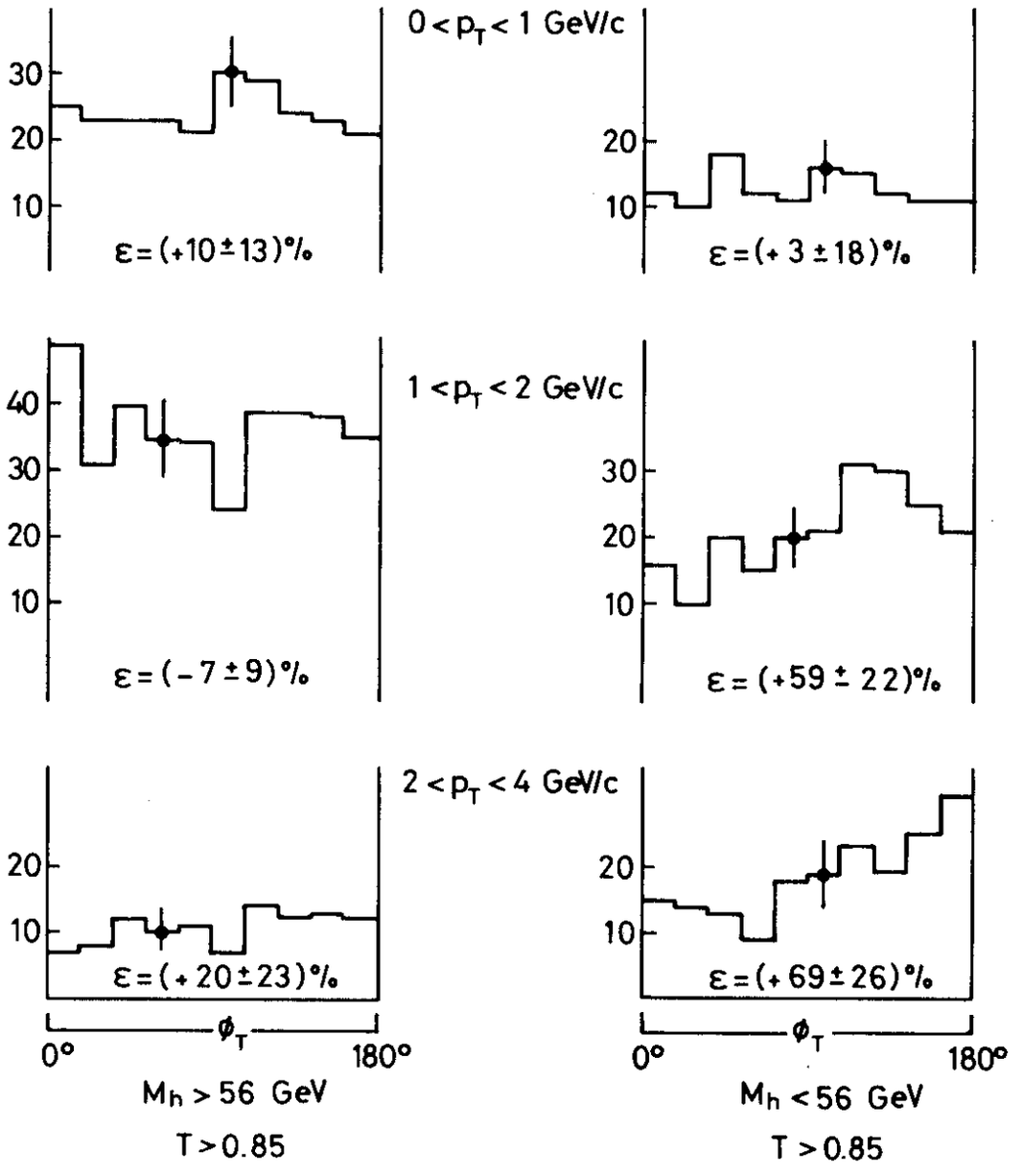
0 < p_T < 1 GeV/c
30
20
10
ε = (+10 ± 13)%
20
10
ε = (+ 3 ± 18)%
1 < p_T < 2 GeV/c
40
30
20
10
ε = (− 7 ± 9)%
30
20
10
ε = (+59 ± 22)%
2 < p_T < 4 GeV/c
20
10
ε = (+ 20 ± 23)%
20
10
ε = (+ 69 ± 26)%
ϕ_T
0°
180°
M_h > 56 GeV
T > 0.85
ϕ_T
0°
180°
M_h < 56 GeV
T > 0.85

Fig. 13